Fan C, Hinkelman K, Fu Y, Zuo W, Huang S, Shi C, et al. Open-source Modelica models for the control performance simulation of chiller plants with water-side economizer. *Applied Energy* 2021;299:117337. https://doi.org/10.1016/j.apenergy.2021.117337.

Open-source Modelica models for the control performance simulation of chiller plants with water-side economizer

Chengliang Fan[a,b], Kathryn Hinkelman[b], Yangyang Fu[c], Wangda Zuo[b], Sen Huang[d], Chengnan Shi[b], Nasim Mamaghani[b], Cary Faulkner[b], Xiaoqing Zhou[a,*]

[a] Guangdong Provincial Key Laboratory of Building Energy Efficiency and Application Technologies, Academy of Building Energy Efficiency, School of Civil Engineering, Guangzhou University, Guangzhou 510006, China

[b] Department of Civil, Environmental and Architectural Engineering, University of Colorado Boulder, Boulder, CO 80309, USA

[c] Department of mechanical engineering, Texas A&M University, College Station, TX 77840, USA

[d] Pacific Northwest National Laboratory, 902 Battelle Blvd, Richland, WA 99354, USA

[*] Corresponding author. E-mail address: zhouxq@gzhu.edu.cn

Abstract

There are several cooling mode control sequences for chiller plants with water-side economizers adopted in industry and academia, and it is widely known that this supervisory control significantly affects energy consumption; however, there is a lack of a modeling resource to allow multiple control sequences to be evaluated systematically under different settings, such as system configurations, load types, and climate locations. To fill this gap, this paper develops open-source Modelica models to simulate the control and energy performance of multiple cooling mode control sequences for chiller plants with water-side economizers. These models allow users to develop and test their advanced control sequences for chiller plants with water-side economizers for their target climates and system configurations. To demonstrate how these models can be utilized, a chiller plant with an integrated water-side economizer is simulated using two advanced cooling mode control sequences, two cooling load types, and six climates, for a total of 24 simulation cases. This study revealed that the energy saving potential varied from 8.6% to 36.8% for constant load profiles in all of the considered climates, and from 6.3% to 25.8% for variable load profiles in most of the climates. Results also showed that the developed system models are able to capture transient control details and reveal counterintuitive energy performance.

Keywords: Chiller plant; Water-side economizer; Modelica; Control sequence; Free cooling

Nomenclature

AHU	Air handling unit	*RA*	Return air
CH	Chiller	*S*	Speed
CHW	Chilled water	*SA*	Supply air
CW	Condenser water	*SUT*	Staging up threshold
COP	Coefficient of performance	*SDT*	Staging down threshold
CHWP	Chilled water pump	*T*	Temperature, ˚C
CWP	Condenser water pump	*WSE*	Water-side economizer
CT	Cooling tower	δt	Elapsed time
$\dot{C}_{min}$	Minimal capacity flow rate		
$\dot{C}_{max}$	Maximum capacity flow rate	*Subscripts*	
DP	Differential pressure	*app*	Approach temperature, ˚C
FC	Free cooling	*fan*	Cooling tower fan
FMC	Full mechanical cooling	*in*	Inlet water
H	Head pressure	*out*	Outlet water
$\dot{m}$	Flow rate of water or air	*off*	Component off
Max	Maximum value	*on*	Component on
Min	Minimum value	*pre*	Predicted temperature, ˚C
N	Number	*ret*	Return temperature, ˚C
OA	Outdoor air	*sup*	Supply temperature, ˚C
P	Power, kW	*set*	Setpoint temperature, ˚C
PF	Performance factor, kW/ton	*tot*	Total
PMC	Partial mechanical cooling	*wb*	Wet-bulb
PLR	Part load ratio	ε	Heat exchanger effectiveness
Q	Cooling load, kW (ton)		

1. Introduction

In a chiller plant with a water-side economizer (WSE), the WSE is a heat exchanger that cools chilled water by condenser water [1]. Often regarded as "free cooling", the WSE takes advantage of the low wet-bulb temperature (T_{wb}) to reduce the cooling needs of chillers [2]. Employing a WSE can decrease the cooling energy consumption by reducing the chiller operating time or increasing the chiller efficiency [3]. Previous studies show that the WSE can reduce the energy consumption of chiller plants up to 40% [4,5].

Although the WSE can reduce the energy consumption of chiller plants, those savings are highly dependent on the control schema and energy consumption of other equipment. Firstly, using a WSE poses control challenges to the operation of chiller plants. Common problems include short cycling of chillers [6], chilled water supply temperature fluctuations [7,8], and room temperatures drifting outside of acceptable ranges. Moreover, using a WSE may cause the chillers to deviate from their optimal performance curves or even shut down unexpectedly when exposed to the colder condenser water temperatures required for the WSE [9]. Additionally, reducing the energy consumption for chillers comes at the expense of increased energy consumption for cooling towers or pumps when the WSE is enabled [10]. At times, this tradeoff causes the total energy consumption of the plant to be higher with a WSE than without one. Due to these challenges, the chiller plant may not function at its optimal state when WSE is enabled. To diagnose these challenges offline and improve the operation of chiller plants with WSE, computational modeling and simulation is highly effective.

While the literature on modeling and simulation of chiller plants with WSE is abundant to be discussed further in Section 2, there is a lack of modeling tools that can evaluate multiple advanced control sequences systematically across plant configurations, load types, and climate locations. In simulation settings and real-world practice, the energy performance of the chiller plant with WSE is usually evaluated with a specific control sequence, one cooling load type, and either a single climate or multiple climates [11,12]. However, the energy performance of chiller plants with WSE depends on many factors, such as equipment sizing, chiller plant configurations, control sequences, climates, and cooling load types [13]. Because of the range of flexibility in these operating conditions, there are nearly unlimited ways these plants can be controlled. Due to the above-mentioned challenges, it is critical that control sequences are assessed across the range of their exposed conditions to realize the energy benefits of WSE.

Thus, the objective of this work is to develop open-source Modelica models for evaluating the energy performance of chiller plants with WSE across multiple control scenarios, such as different system configurations, control sequences, cooling load types, and climates. This allows users to systematically test their control sequences across the range of their site conditions and more appropriately select and tune their sequences for each target site. Modelica is an equation-based, object-oriented modeling language for modeling multi-domain physical systems with dynamic behaviors [14,15]. It was selected because of the rich open-source libraries available, its ability to model both the mechanical and control systems in one platform, and its suitability to simulate the performance of control sequences by capturing both the fast transient responses of control actions

and slow dynamic responses of thermofluid systems [16,17]. Contrary to previous works, these open-source models are designed to accept a wide range of control scenarios, suitable for chiller plants with WSE in any climate globally.

The rest of this paper is organized as follows. Previous literature in modeling and simulation of chiller plants with WSE are detailed further in Section 2. Then, the open-source Modelica implementation – including the cooling system models, control models, post-processing models and integrated system simulation model – is presented in Section 3. In Section 4, a case study including 24 model combinations demonstrates the flexibility and suitability of this tool to evaluate the control performance of chiller plants with WSE. One common system configuration, two control sequences from literature, two load types, and six climates in the U.S. are used for demonstration. The system performances in terms of control stability and energy consumption are presented and analyzed in Sections 5 and 6, before concluding this contribution in Section 7.

2. Literature review

This section presents the past literature on modeling and simulation of chiller plants with WSE. With the goal of this work being to evaluate a range of chiller plant with WSE designs, the variety of plant configurations are first discussed. Then, the range of available modeling tools will be presented, followed by the past works in simulating chiller plants with WSE.

Chiller plants with WSE can be configured in many different ways in practice [18]. When the WSE is in series with the chillers on the chilled water side, it is often referred as an integrated WSE [19,20]. This means that the WSE can meet all or some of the cooling load while the chillers meet the remainder. Conversely, chillers and WSE can also be in parallel (or nonintegrated) with the chillers on the chilled water side [21,22]. This means that the economizer operates when it can meet the entire load independently of the chillers [8]. Further, WSE and chillers can also be in parallel or series on the condenser water side [23]. The collected WSE configurations of chiller plants with WSE from literature are summarized in Appendix A. Among those, the configuration with a series chiller-WSE connection on the chilled water side (integrated) and a parallel chiller-WSE connection on the condenser water side is the most common in the literature since it often has higher energy efficiency than other configurations [5,7,9]. This configuration is implemented and studied in this paper as a demonstration of the proposed simulation model.

Several modeling tools have been used to evaluate the energy and control performance of chiller plants with WSE. For example, Ham and Jeong [19] used EnergyPlus to simulate the energy performance of the chiller plant with integrated WSE. Some control models are idealized in EnergyPlus and cannot fully reflect the actual response and transient dynamics of system operation [3]. For instance, control signal and components actions usually lack delay time and waiting time in EnergyPlus [24,25]. Some studies [26,27] developed chiller plants with WSE models as well as their controls using TRNSYS to simulate and evaluate the energy performance of the plant, while others used TRNSYS to simulate the chiller plant with WSE and developed the control strategy in MATLAB [28]. MATLAB/Simulink are powerful tools for computing; however, they are not priorities for modeling multi-physics dynamic analysis [29]. Additionally, some tools can model system dynamics but often have problems when the simulated system has a mixture of fast and

slow dynamics (aka “stiff” problems) [30], which is common of this application. Díaz, Cáceres, Torres, Cardemil and Silva-Llanca used Engineering Equation Solver to estimate energy consumption for the chiller plant with WSE in multiple locations [5]. However, the developed chiller plant models usually lack flow resistance models with pressure drop for equipment and pipelines. The resulted models do not consider the dynamic pressure distribution characteristics in water loops [31]. Contrary to the limitations mentioned above, the developed Modelica-based chiller plant with WSE models in this study take advantage of the equation-based object-oriented Modelica-based modeling features, such as its flexibility to model different system configurations, control sequence and local controls and its adaptability to implement implicit variable timestep solvers which can efficiently simulate fast and slow dynamic processes that are critical in control evaluation [32]. Thus, Modelica-based modeling approach is selected for this work.

Many studies are devoted to simulating and evaluate the energy performance of chiller plans with WSE. Wei, Li, Shi and Li [26] simulated WSE performance with a variable T_{wb} setpoint control, which extended the operating hours in free cooling mode and reduced total energy consumption by 7% compared to the conventional constant T_{wb} control method. Durand-Estebe, Le Bot, Mancos and Arquis [28] simulated chiller plants with WSE operation with a temperature-adaptive control strategy, which can reduce the energy consumption of chiller plants up to 50%. Taylor [7] and Stein [9] proposed their control sequences to achieve more WSE operation time. Agrawal, Khichar and Jain [27] evaluated the energy of chiller plants with WSE with a condenser water supply temperature control strategy, that can reduce energy consumption by 30%. Díaz, Cáceres, Torres, Cardemil and Silva-Llanca [5] analyzed the effect of climates on the thermodynamic performance of a chiller plant with WSE. They found that chillers’ energy saving is limited in desert climate since it prevents implementing WSE operation. Cheung and Wang [33] simulated energy performance of the specific control sequence for chiller plants with WSE under multiple climates. The results show that the different system configurations can reduce the annual energy consumption by 3-15% depending on the climates. Although the above studies have evaluated the energy performance of chiller plants with WSE in simulation or even in practice, they lack flexibility in evaluating multiple control sequences under several design and climate conditions. Thus, this work aims to suit this purpose.

3. Model implementation

This section first introduces the Modelica models’ implementation of the chiller plant with WSE for equipment and controls. The chiller plant models consist of individual equipment and subsystem models that are introduced in Section 3.1. The equipment, subsystem, and system models were developed hierarchically for isolation testing and improved reusability. The control models similarly include equipment-level and system-level controls and are introduced in Section 3.2. The supervisory control and local control models are integrated at the top-level, allowing their seamless replacement. Then, the complete system models are developed by coupling the plant model with control models in Section 3.3. This allows control engineers to test a variety of advanced control sequences under one single platform. Also, models for post-processing are included to analyze the system operation and energy consumption.

3.1 Cooling system

3.1.1 Equipment models

A chiller plant with WSE usually includes water-cooled chillers, WSE, cooling towers, chilled water pumps, condenser water pumps, valves, distribution pipes, etc. The chiller, pump, valve, and pipe models are modeled using the basic models available in the Modelica Buildings Library [16]. In addition, this paper implements the cooling tower model based on Merkel's theory in Modelica environment to calculate the total heat transfer between the air and water entering the tower. The fundamental basis for Merkel's theory is that the steady-state total heat transfer is proportional to the difference between the enthalpy of air and the enthalpy of air saturated at the wetted-surface temperature [34,35]. This paper has open-source released the Merkel cooling tower in the Modelica Buildings Library (v7.0.0). The vectorized models for identical chillers and pumps are created based on basic models from the Modelica Buildings Library. The vectorized models are then connected in parallel and share the same inputs and outputs nodes. A new WSE model is also developed, which mainly consists of a plate heat exchanger model with constant effectivity, a valve model, and an outlet temperature control block.

Performance equations of the chiller plants are summarized in Table 1. The chiller performance is usually affected by three equations: *CFT*, *EIRFT*, and *EIRFPLR*. *CFT* is available cooling capacity as a function of the chilled water supply temperature ($T_{sup,CHW}$) and leaving condenser water temperature ($T_{ret,CW}$), *EIRFT* represents the full load efficiency as a function of the $T_{sup,CHW}$ and $T_{ret,CW}$, and *EIRFPLR* represents the efficiency as a function of the part load ratio (*PLR*). For chilled water pumps, condenser water pumps, and cooling tower fans, the head pressure (*H*) and power (*P*) of these components are represented as a quadratic equation in terms of the flowrate. The mass flow rate of water or air is represented by $\dot{m}$, while b, c, d, e, and f are the coefficients of each parameter. For the cooling tower heat transfer process, Q is the total cooling load capacity, NTU is number of transfer units, $\dot{C}_{min}$ is the minimal capacity flow rate, $\dot{C}_{max}$ is the maximum capacity flow rate, $T_{CW,in}$ is the inlet condenser water of cooling tower, $T_{wb,in}$ is wet-bulb temperature of the inlet air, and ε is heat exchanger effectiveness [36].

Table 1 Performance equations for chiller plant's main equipment.

Equipment	Performance equation
Chiller	$CFT = b_1 + b_2 T_{sup,CHW} + b_3 T_{sup,CHW}^2 + b_4 T_{ret,CW} + b_5 T_{ret,CW}^2 + b_6 T_{sup,CHW} T_{ret,CW}$
	$EIRFT = c_1 + c_2 T_{sup,CHW} + c_3 T_{sup,CHW}^2 + c_4 T_{ret,CW} + c_5 T_{ret,CW}^2 + c_6 T_{sup,CHW} T_{ret,CW}$
	$EIRFPLR = d_1 + d_2 T_{ret,CW} + d_3 T_{ret,CW}^2 + d_4 PLR + d_5 PLR^2 + d_6 T_{ret,CW} PLR + d_7 PLR^3$
Fan/Pump	$H = e_1 + e_2 \dot{m} + e_3 \dot{m}^2$
	$P = f_1 + f_2 \dot{m} + f_3 \dot{m}^2$
Cooling tower	$\varepsilon = \frac{1 - exp\{-NTU[1 - (\dot{C}_{min}/\dot{C}_{max})]}{1 - (\dot{C}_{min}/\dot{C}_{max}) exp\{-NTU[1 - (\dot{C}_{min}/\dot{C}_{max})\}}$

$$Q = \varepsilon \dot{C}_{min}(T_{CW,in} - T_{wb,in})$$

3.1.2 Subsystem models

Different subsystems can be modeled using a hierarchical approach. For example, the chiller model and WSE model can be packaged together to create a chiller with WSE model. This package can later be inherited to design the entire plant. To complete the chiller plant with WSE subsystem model, other instances such as bypass valves and pumps are added, inputs and outputs for the model are exposed, and the components are connected appropriately. Fig. 1 shows the subsystem configuration of a series chiller-WSE connection on the chilled water side and a parallel chiller-WSE connection on the condenser water side. The blocks on the left represent the model inputs, including the on/off signal for chillers, pumps and WSE, supply chilled water temperature set point signal, bypass valve position signal, and pump speed signal from different controllers. On the right are the model outputs, such as WSE supply chilled water temperature, chiller power, and pump power.

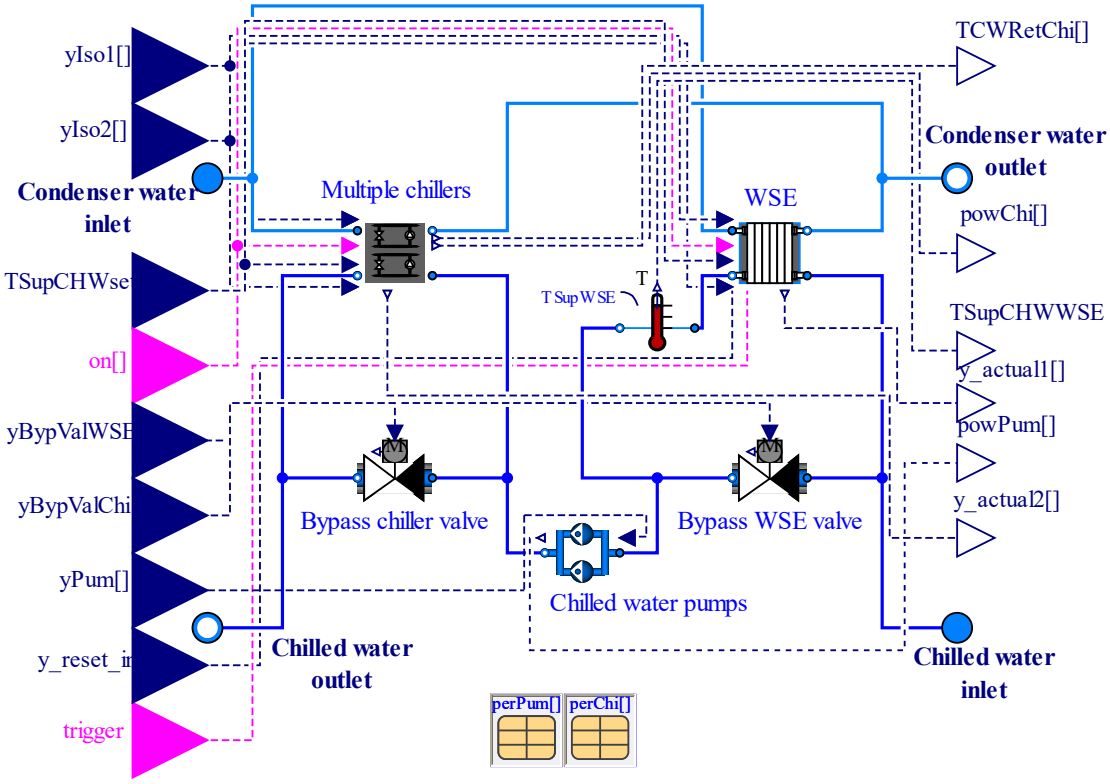

Fig. 1. Model implementation of chiller plant with integrated WSE.

3.2 Control system

3.2.1 Equipment-level control models

The equipment-level control logics of a chiller plant with WSE are summarized in Table 2, including staging control (e.g., cooling tower staging control, chiller staging control, WSE staging control, and water pump staging control), speed control (e.g., cooling tower fan speed control,

water pump speed control), isolation valve control, and bypass valve control. In Table 2, variable $\delta t_{stage,on}$ is the elapsed time since the equipment was activated, δt_{min} is the minimum waiting time threshold, SUT is staging up threshold, SDT is staging down threshold, $S_{CW,min}$ is the minimum CW pump speed, and PID_{CW} is the PID controller output signal for modulating DP_{CW}. Since the equipment sizes are all identical with each other, the control logics and parameter setpoints can be considered the same based on the engineering practice. Thus, it is assumed that cooling towers are controlled to the same condenser water set point, chillers are controlled to the same chilled water set point, and pumps are controlled to the same speed settings.

Table 2 Equipment-level control logics.

Equipment	Control type	Control logic
Chiller	Staging	Chillers stage up: $\delta t_{stage,on}\ and\ PLR_{CH} > SUT\ for\ \delta t_{min}$ Chillers stage down: $\delta t_{stage,on}\ and\ PLR_{CH} < SDT\ for\ \delta t_{min}$
	Chiller bypass	FC mode: fully open PMC and FMC modes: modulate DP_{CH} at set point
CHW pump	Staging	CHW pumps stage up: $\delta t_{stage,on}\ and \frac{\dot{m}_{CHWP}}{\dot{m}_{CHWP,nominal}} > SUT\ for\ \delta t_{min}$ CHW pumps stage down: $\delta t_{stage,on}\ and \frac{\dot{m}_{CHWP}}{\dot{m}_{CHWP,nominal}} < SDT\ for\ \delta t_{min}$
	Speed	Modulate DP_{CHW} at its set point
Cooling tower	Cell staging	CT stages up: $\delta t_{stage,on}\ and \frac{\dot{m}_{CWP}}{\dot{m}_{CWP,nominal}} > SUT\ for\ \delta t_{min}$ CT stages down: $\delta t_{stage,on}\ and \frac{\dot{m}_{CWP}}{\dot{m}_{CWP,nominal}} < SDT\ for\ \delta t_{min}$
	Speed	FC mode: launch from 100% and maintain $T_{sup,CHW}$ at its set point PMC and FMC modes: maintain $T_{sup,CW}$ at its set point
CW pump	Staging	FC mode: CW pump stages on when $S_{CT} > staUpThr\ for\ \delta t_{min}$, CW pump stages down when $S_{CT} < staDowThr\ for\ \delta t_{min}$ PMC and FMC modes: $N_{CWP} = N_{CH}$
	Speed	FC mode: $Max\ (S_{CT}, S_{CW,min})$ PMC and FMC modes: $Max\ (PID_{CW}, PLR_{CH}, S_{CW,min})$
WSE	WSE bypass	FC and PMC modes: Modulate DP_{CHW} at set point FMC mode: fully open

3.2.2 System-level control models

Supervisory control strategies include cooling mode control sequences, a chilled water supply temperature ($T_{sup,CHW}$) reset control, a chilled water loop differential pressure (DP_{CHW}) reset control, and a condenser water supply temperature ($T_{sup,CW}$) reset control. Both $T_{sup,CHW}$ and DP_{CHW} set points are reset based on coil control valve positions. A single reset control method is used to control both set points [9]. The reset strategy is first to increase the differential pressure DP_{CHW} to increase the mass flow rate. If DP_{CHW} reaches the maximum value and further cooling is still needed, $T_{sup,CHW}$ set point is gradually reduced. If there is too much cooling, $T_{sup,CHW}$ set point and DP_{CHW} will be changed in the reverse direction [37]. A $T_{sup,CW}$ reset control is summarized in Table 3. When the chiller plant system operates in FC cooling mode, the $T_{sup,CW}$ is free-floating and avoids freezing. In PMC mode, $T_{sup,CW}$ is set as the predefined value. In FMC mode, $T_{sup,CW}$ is controlled based on an approach temperature method.

Table 3 Supply condenser water temperature reset control.

Cooling mode	Reset logic
FC	$T_{sup,CW}$ setpoint is free-floating
PMC	$T_{sup,CW}$ is reset to a predefined value
FMC	$T_{sup,CW}$ is reset using $T_{wb} + T_{app,CT,pre}$

Any advanced control sequence can be implemented in the developed testbed using elementary blocks from the Modelica Buildings Library. The implemented CWST-based control sequence in Modelica is selected as an example, as shown in Fig. 2. There are four types of blocks in each sequence controller. On the left are the connectors of the input control signals expressed as real numbers, including $T_{sup,CW,WSE}$, $T_{ret,CHW,WSE}$, $T_{sup,CHW,set}$, etc. Next to those are blocks for calculating temperature difference. Continuing to the right are the implemented control logics of the state graph, including control delay time and equipment waiting time. The transitions between the cooling mode states are represented by the horizontal black bars, and each transition has unique preceding and succeeding states. On the far right are output signal connectors, which output the cooling mode control signal.

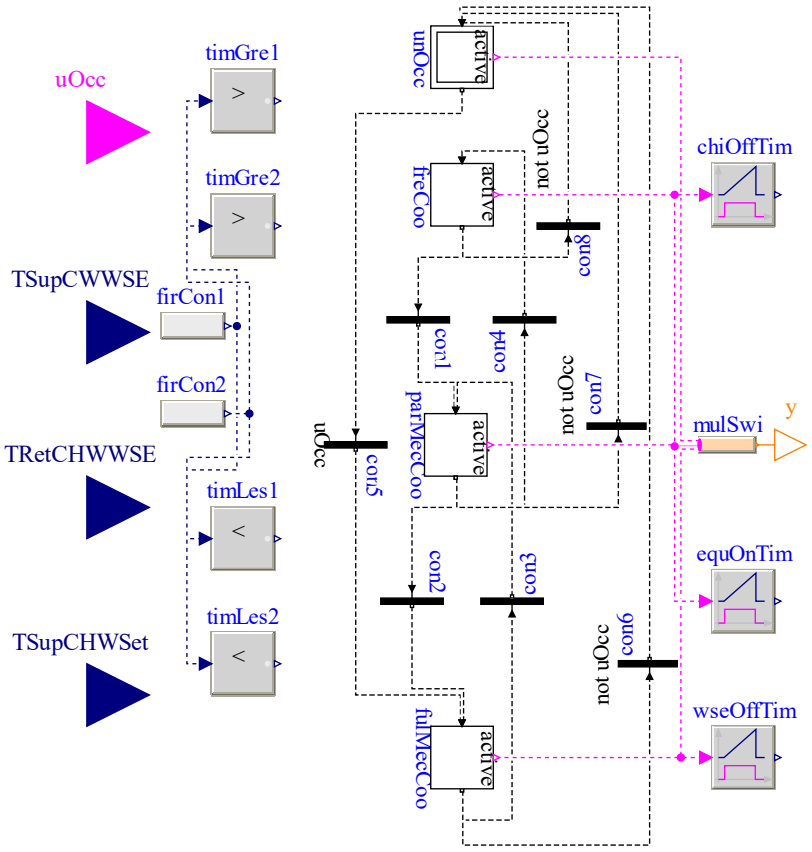

Fig. 2. Diagram of a CWST-based control sequence model.

3.3 Integrated control and system models

In the developed Modelica system model, the equipment, subsystem, and system models are developed hierarchically, while the flat control sequences are integrated at the top-level, allowing their seamless replacement by the user. This allows control engineers to test a variety of advanced control sequences under multiple climates using one single system model. Fig. 3 shows an example of the complete model of a chilled water system with WSE, which is coupled with the CWST-based control sequence. The dashed line represents the control signal line, and the double solid line is the fluid line. This model consists of three parts: the control system, the cooling system, and post-processing. The left side is the control system, which includes the system-level supervisory control and the equipment-level local control. In the middle is the cooling system, including the developed chiller plant with integrated WSE model and other component models (e.g., room model, pipes resistance model, and AHU model). The right side is the post-processing, which is used to calculate the energy consumption.

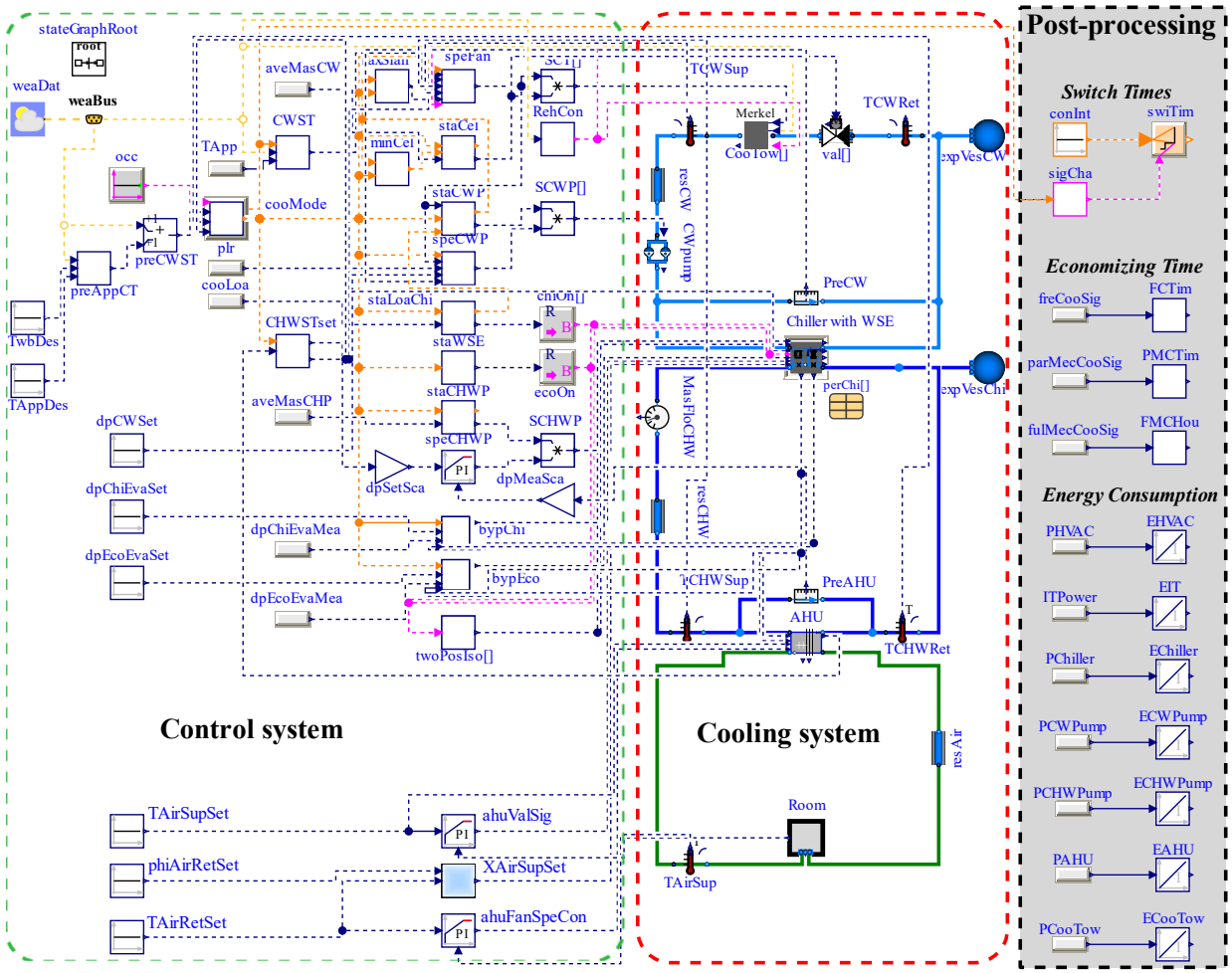

Fig. 3. Top-level model diagram for the chiller plant with integrated WSE.

4. Case study

A total of 24 simulations are performed to demonstrate the flexibility of the developed open-source models and provide an example for how control engineers can simulate their control sequences using this computational testbed. While the same chiller plant with WSE configuration is used across all simulations, the control sequence, load type, and climate location varies, as summarized in Table 4. The six representative ASHRAE climate zones are selected from hot and dry (2B) to cold and moist (6A), to cover a wide spectrum of temperature and moisture conditions. This section presents the case study system description and model settings, including the climate, load configurations, and cooling mode control sequences.

Table 4 System configuration variables across all simulation cases.

Types	Description	Content
Location	Climate zones	Tucson, AZ (2B hot and dry); Atlanta, GA (3A warm and moist); San Francisco, CA (3C warm and marine);

		Seattle, WA (4C mixed and marine); Denver, CO (5B cool and dry); Rochester, NY (6A cold and moist)
Cooling load	Profile type	Constant / Variable
Control sequences	Cooling mode control	two control sequences

4.1 Plant configuration

There are usually five types of configurations for chiller plants with WSE in other studies, as shown in Appendix A. The modeled plant, shown in Fig. 4, is a common water-cooled chiller plant with an integrated WSE, where the WSE is in parallel will the chillers on the condenser water side. There are usually three cooling modes for chiller plants with integrated WSE: (1) free cooling (FC) mode, where only the WSE is on; (2) partial mechanical cooling (PMC) mode, where the chillers and WSE are both running; and (3) full mechanical cooling (FMC), where only the chillers are on. Different cooling modes are achieved by adjusting valve positions. For the studied system, in FC mode, chiller isolation valves (V_{1_1}, V_{1_2}, V_{2_1}, and V_{2_2}) are closed, while WSE isolation valves (V_3 and V_4) and chiller bypass valve V_6 are open, WSE bypass valve V_5 is modulated to maintain *DP* across WSE at a set point. In PMC mode, V_{1_1}, V_{1_2}, V_{2_1}, V_{2_2}, V_3, and V_4 are open, while V_5 and V_6 are modulated to maintain *DP* across WSE and chillers at their set points. In FMC mode, V_3 and V_4 are closed, while V_{1_1}, V_{1_2}, V_{2_1}, V_{2_2}, V_5 are open, V_6 is modulated to maintain *DP* across chillers at the set point.

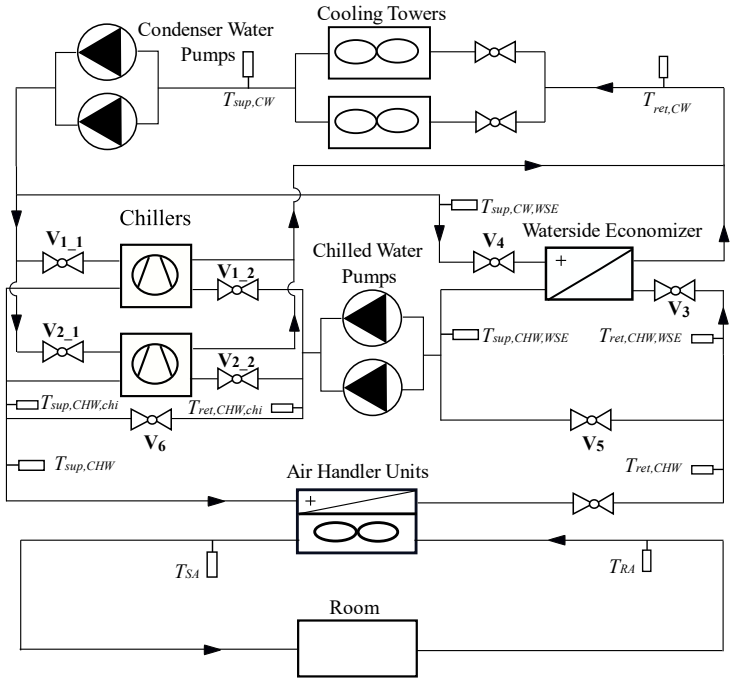

Fig. 4. Configuration of a chiller plant with integrated WSE in parallel connection on condenser water side.

The sizing of the system is held constant across all simulation scenarios in this study. The design temperature differences of the chilled water loop, condenser water loop, and air loop are 10 ˚C,

7.5 °C, and 8.9 °C, respectively. The design chilled water supply temperature, condenser water supply temperature, and supply air temperature are 7.8 °C, 25.5 °C, and 17.8 °C, respectively. The system is tested under constant load and variable load, as discussed in Section 4.3. The chillers, pumps, cooling towers, and air handling units are sized accordingly based on the design cooling load [38]. Further information on the equipment's nominal sizing can be found in Appendix B.

4.2 Control sequences

The publicly released cooling mode control sequences can generally be classified into two categories: the condenser water supply temperature (CWST)-based control sequences and the chilled water supply temperature (CHWST)-based control sequences. Two advanced control sequences have been selected from the existing literature to demonstrate the system model's ability to include detailed control logics for chiller plants with WSE: a CWST-based control sequence and a CHWST-based control sequence. The CWST-based control sequence is from Griffin [39]. In this sequence, condenser water supply temperature is regarded as the main control parameter to decide the cooling mode transition strategy. The CHWST-based control sequence is from Taylor's study [7]. In this sequence, chilled water supply temperature of WSE is regarded as the main control parameter to decide on cooling mode transition strategy. While these two sequences (as shown in Appendix C) are selected to demonstrate the available flexibility of the open-source models, users can evaluate other control sequences using this platform.

The final combination of each system is summarized in Table 5. For example, the chiller plant coupled with a CWST-based control sequence under constant load is named CWST-C. To investigate the energy saving potential of the chiller plant with WSE, the energy use of the plant without WSE is considered as the baseline. The energy consumption of air handling units is not usually considered in chiller plant energy consumption studies and hence is not included in this study as well.

Table 5 Combinations of chiller plant with WSE under different sequences and load types.

Control sequence	Cooling load type	Abbreviation
CWST-based	Constant	CWST-C
	Variable	CWST-V
CHWST-based	Constant	CHWST-C
	Variable	CHWST-V

4.3 Load types

Two load types (constant load and variable load) are applied to simulate the performance of the system model. The constant cooling load is represented by a data center with 2160 kW (615 tons) load, a common energy-intensive application for chiller plants with WSE. The variable cooling load represents an office building with a data center. The cooling load distributions for this load type are 40% (864 kW) for the data center and 60% (1296 kW) for the office building so that the total peak load is 2160 kW. EnergyPlus is used to generate the variable cooling load profile.

4.4 Validation

The validation process includes two levels, one is for individual equipment, and the other one is for the cooling system. All major equipment, such as chillers, pumps, and air handling unit, have been validated. Individual cooling equipment have been calibrated with measured data from a real data center cooling system; these results are available in previous publications belong to the authors of this paper [10,40]. The implemented Merkel's theory-based cooling tower model in Modelica is validated with the equivalent cooling tower model available in EnergyPlus.

To validate the cooling system model, a baseline model is established by EnergyPlus to predict the energy performance. The benchmark model uses the same design parameters as the Modelica model, both with the constant cooling load scenario. The predicted site annual energy consumption for the two models is in good agreement, with relative differences ranging from -6.4% to 0.9% in the six locations, as shown in Table 6.

Table 6 Relative difference in energy consumption of cooling system.

Climate Zone	Energy consumption (MWh)		Relative
	EnergyPlus	Modelica	difference (%)
2B	6077.1	5932.5	-2.4
3A	6266.1	5965.9	-4.8
3C	6243.9	6127.1	-1.9
4C	5954.8	5576.7	-6.3
5B	5093.0	5137.4	0.9
6A	5421.0	5179.1	-4.5

4.5 Performance metrics

To ensure that the system is functioning as designed, two system control performance indicators ($T_{sup,CHW}$ and T_{SA}) are selected. These two temperature indicators are fundamental to a correctly functioning cooling system. A chilled water supply temperature, $T_{sup,CHW}$, that is held within acceptable tolerances of its setpoint will allow the air handling unit to perform properly. The supply air temperature is similarly critical, as it is the air supplied to building zones to meet the cooling needs.

Further, the energy performance of chiller plants with WSE under various control sequences is reported and evaluated. The chiller plant efficiency is represented as kW/ton and is defined as the ratio of chiller plant power consumption to total cooling load, which is a common performance factor (*PF*) used for chiller plant energy performance analysis [41,42]. This can be represented as:

$$PF = \frac{P_{CH}+P_{CHWP}+P_{CWP}+P_{CT}}{Q_{tot}} \quad (1)$$

where P_{CH}, P_{CHWP}, P_{CWP}, and P_{CT} are the power consumption (in kW) of chillers, chilled water pumps, condenser water pumps, and cooling towers, respectively, and Q_{tot} is the total cooling load (in ton). A lower kW/ton corresponds to less energy being consumed by the chiller plant while still satisfying the cooling load. Thus, the smaller the kW/ton, the higher the energy performance of the chiller plant.

5. Results

This section presents the results of the 24 simulation cases (1 system configuration, 2 control sequences, 2 load types, and 6 climates). To evaluate the control system, the system performances in terms of control stability and energy consumption are analyzed in Section 5.1 and 5.2.

5.1 Control performance

Analyzing the selected control indicators, $T_{sup,CHW}$ and T_{SA}, for the studied cases revealed that the set points are met at most times. However, there are few dynamic transient behaviors, as shown in Fig. 5 (a). $T_{sup,CHW}$ may be beyond the set point because of chiller turning on events and the dead band temperature of the control sequences. For example, when the chiller turns on at 8 a.m. due to the increased cooling load reflected by PLR, it causes an upward spike for $T_{Sup,CHW}$ that dissipates quickly, as shown in Fig. 5 (b). Similarly, T_{SA} could have an upward spike because of the $T_{sup,CHW}$ upward spike and chilled water pump turning off. For instance, as shown in Fig. 5 (c), turning off the chilled water pump around 11 p.m. can lead to a downward spike of the chilled water flow rate, which causes an upward spike of T_{SA}.

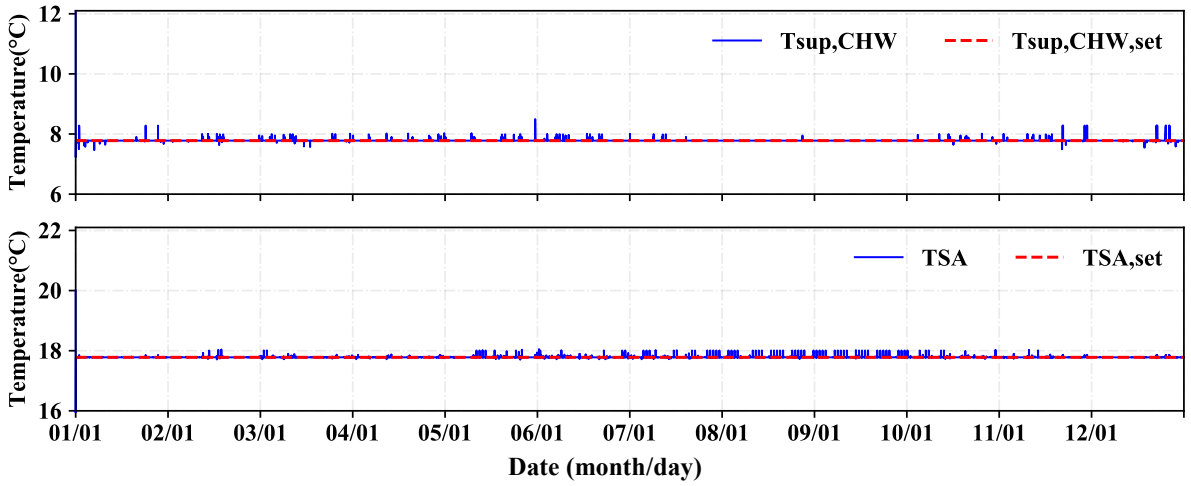

(a) Annual $T_{sup,CHW}$ and T_{SA} results of CWST-V in 3C (San Francisco)

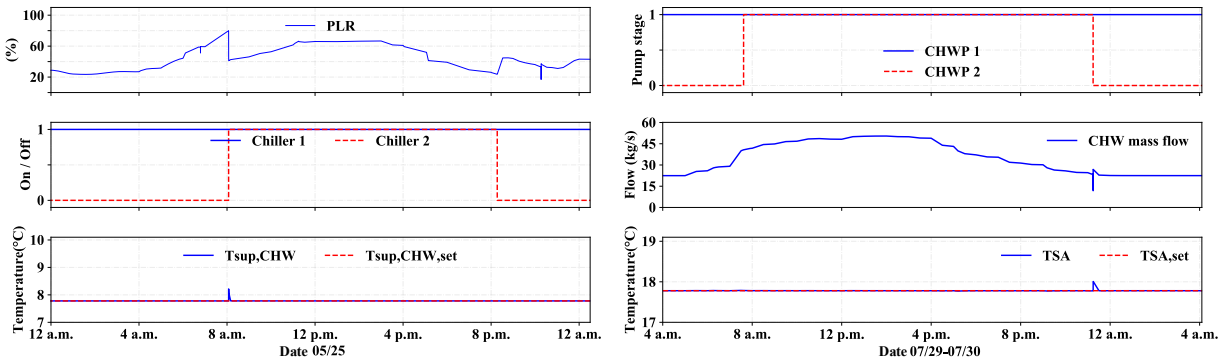

(b) $T_{sup,CHW}$ upward spike (c) T_{SA} upward spike

Fig. 5. Dynamic transients of chilled water supply temperature and supply air temperature.

5.2 Energy performance

This section represents detailed energy performance simulation results and illustrates how the simulation output of the developed testbed can be interpreted by its users. First, the energy consumption of CWST-C system in San Francisco is selected and shown as example in Section 5.2.1. The comprehensive energy performance results across all simulation scenarios under the constant load (Section 5.2.2) and variable load (Section 5.2.3) are shown next. Finally, some unexpected energy results in various climate conditions are presented in Section 5.2.4.

5.2.1 Analysis of CWST-C system in San Francisco

Fig. 6 shows the monthly energy consumption for each equipment. Chiller energy consumption is the highest in the summer season and increases with the monthly averaged T_{wb}. Cooling tower energy consumption is the highest in winter months because the chiller plant often runs in FC or PMC modes during this season. As a result, the cooling tower fan tends to run at higher speeds to provide cold condenser water. This will lead to higher tower energy consumption in winter than in summer, which is reflected in the chart below.

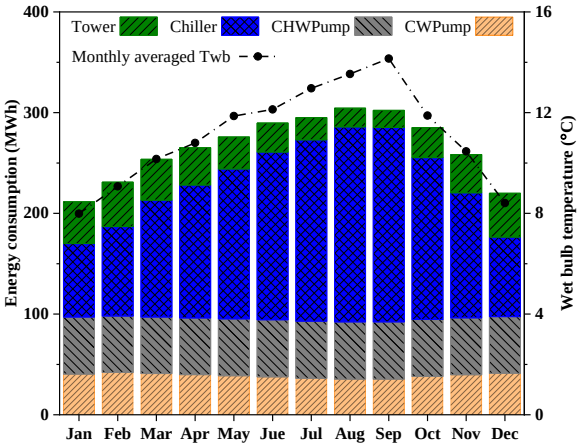

Fig. 6. Monthly equipment energy consumption of CWST-C.

Fig. 7 shows the system energy performance for a week during winter and a week in summer season. As shown in Fig. 7 (a), the cooling mode moves from FMC mode to FC mode, and T_{wb} gradually decreases. The chiller power varies with T_{wb} and is significantly more than the power consumption of the other equipment in FMC mode. Depending on T_{wb}, the cooling tower power may be higher or lower than the chiller in PMC mode. The total power of the chiller plant usually decreases from FMC mode to PMC mode and FC mode, with the least power in the FC mode. The chiller plant kW/ton decreases from 0.65 (COP 5.41) in FMC mode to 0.22 (COP 15.98) in FC mode. Fig. 7 (b) shows that the plant remains in FMC mode during the summer week and the total power slightly varies due to changes of T_{wb}. The energy performance of the chiller plant also has a more substantial fluctuation in winter than in summer because of the large temperature difference in winter. For example, T_{wb} fluctuates between 1 ˚C and 14 ˚C in winter, while it keeps between 12 ˚C and 16 ˚C in summer.

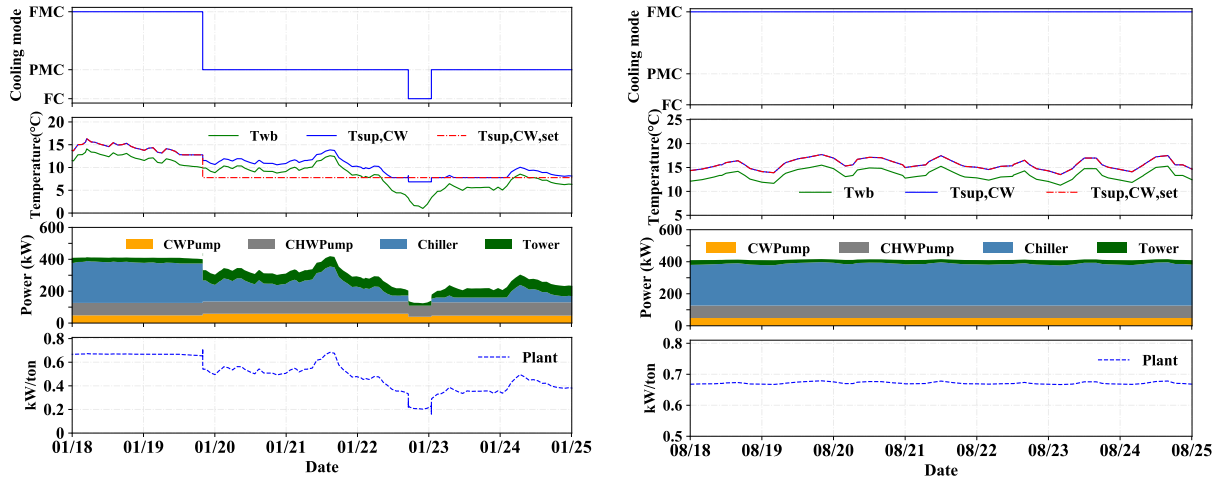

(a) Winter week

(b) Summer week

Fig. 7. Details of the energy performance of CWST-C during a winter week and a summer week.

5.2.2 Energy performance under a constant load profile

Fig. 8 presents the annual energy performance of the chiller plant with/without WSE under constant load profiles. The chiller plant without WSE is set as baseline model to investigate the energy saving potential of the WSE. The total energy consumption of the plant without WSE similar in all six climates, and the total energy consumption for the plant with WSE is notably lower than the plant without WSE. The WSE provides the most energy savings in the cool and dry climate (5B) and the cold and moist climate (6A). While it is less effective in the warm and marine climate (3C), having a WSE still proves beneficial. Compared to a chiller plant without WSE, the energy saving potential of a chiller plant with WSE varies from 8.6% (3C) to 36.8% (5B and 6A).

With WSE, chiller plant kW/ton can be divided into two categories. One is from 0.55 to 0.59 (corresponding to a COP of 6.37 to 5.96) in hot or warm climates (2B, 3A, and 3C), and the other is from 0.41 to 0.49 (corresponding to a COP of 8.58 to 7.18) in mixed, cool, or cold climates (4C, 5B, and 6A). The energy saving mainly comes from the savings in chillers and cooling towers

although the overall chiller plant energy consumption is largely contributed by the chillers and pumps. With WSE, chiller energy can be reduced about 29% to 33% for hot and dry climate (2B) and warm climates (3A and 3C). The most savings that achieved from chiller energy (about 49% - 61%) comes from mixed to cool and cold climates (4C, 5B, and 6A). The chiller energy saving in these cases is at the cost of more energy consumption by cooling towers. The cooling tower energy increase is significant in marine climate (e.g., 3C and 4C) because of the relatively high wet-bulb temperature. Pumps (CW pumps and CHW pumps) usually use similar amounts of energy regardless of climate since their energy is less affected by weather conditions.

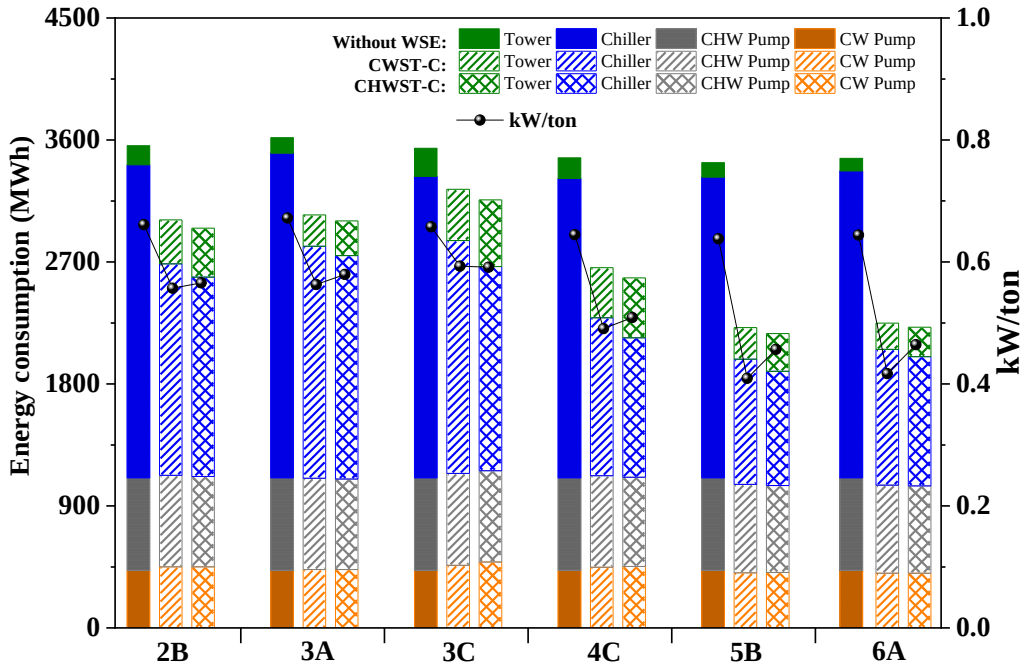

Fig. 8. Energy performance of chiller plant with WSE under constant load in six climates.

Fig. 9 shows the monthly kW/ton of chiller plant with WSE under constant load. The kW/ton results fluctuate with the monthly averaged T_{wb} and usually reach a maximum in July or August. When the monthly averaged T_{wb} is below 7.8 ˚C in cold months (e.g., Jan, Feb, Nov, and Dec), CWST-based control sequence has the least kW/ton in six climates. For hot months (e.g., June, July, and August), the chiller plant kW/ton of two sequences have no obvious differences.

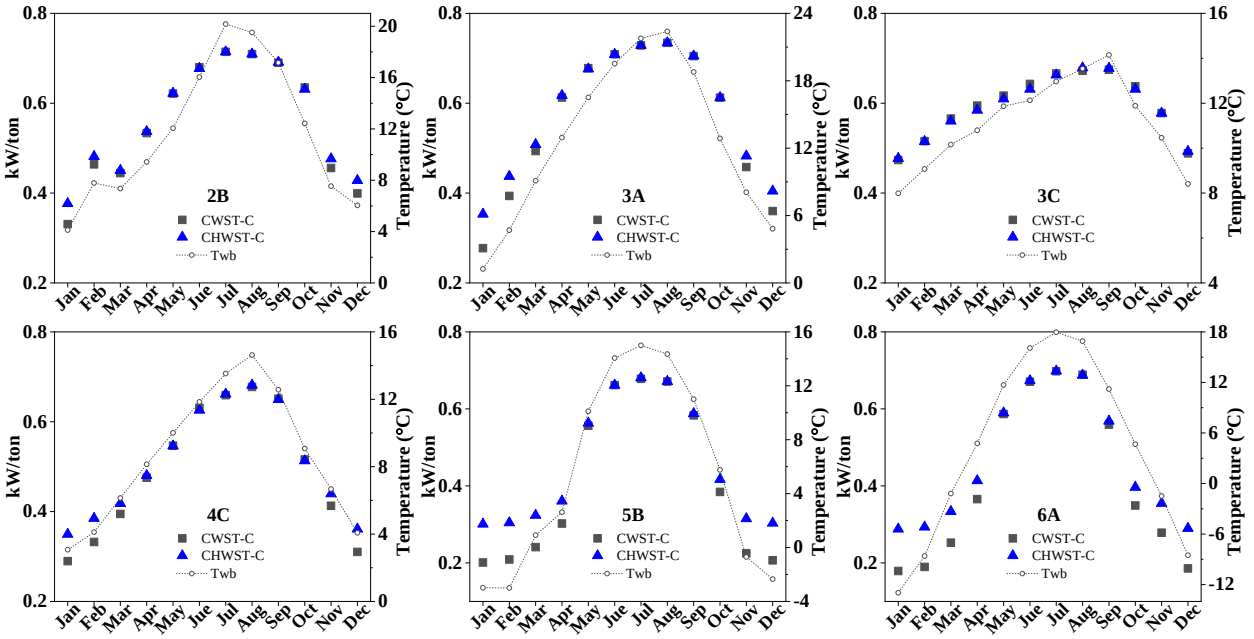

Fig. 9. Monthly chiller plant with WSE kW/ton under constant load.

5.2.3 Energy performance under a variable load profile

Fig. 10 shows the annual energy performance of the chiller plant with WSE under variable load profiles. In general, WSE can provide the most energy saving in the cool and dry climate (5B) and the cold and moist climate (6A), while it is less effective in the hot or warm climates (2B and 3A). Compared to a chiller plant without WSE, the energy saving potential of the plant with WSE varies from 6.3% (2B) to 25.8% (5B and 6A) in the six climates, except 3C (San Francisco), where there was extra energy use of cooling towers caused by a low fixed $T_{Sup,CW}$ set point in PMC mode. This issue is analyzed in Section 5.2.4.

With WSE, the chiller plant kW/ton results are divided into two categories. One is from 0.54 to 0.60 (corresponding to a COP of 6.51 to 5.86) in hot or warm climates (2B, 3A, and 3C), and the other is from 0.40 to 0.47 (COP from 8.79 to 7.48) in the mixed, cool or cold climates (4C, 5B, and 6A). Like the chiller plant with WSE under constant load, the energy saving of the plant with WSE under variable load mainly comes from the savings in chillers. With WSE, the energy consumption of chillers reduces about 23-54% in six climates. The chiller energy saving is at the cost of more energy by cooling towers. The cooling tower energy increase is significant in marine and cool climates (3C and 4C). Cooling tower energy use increased about 238% - 510% compared to the baseline because the cooling tower fan tends to run at a high-speed ratio when WSE is available.

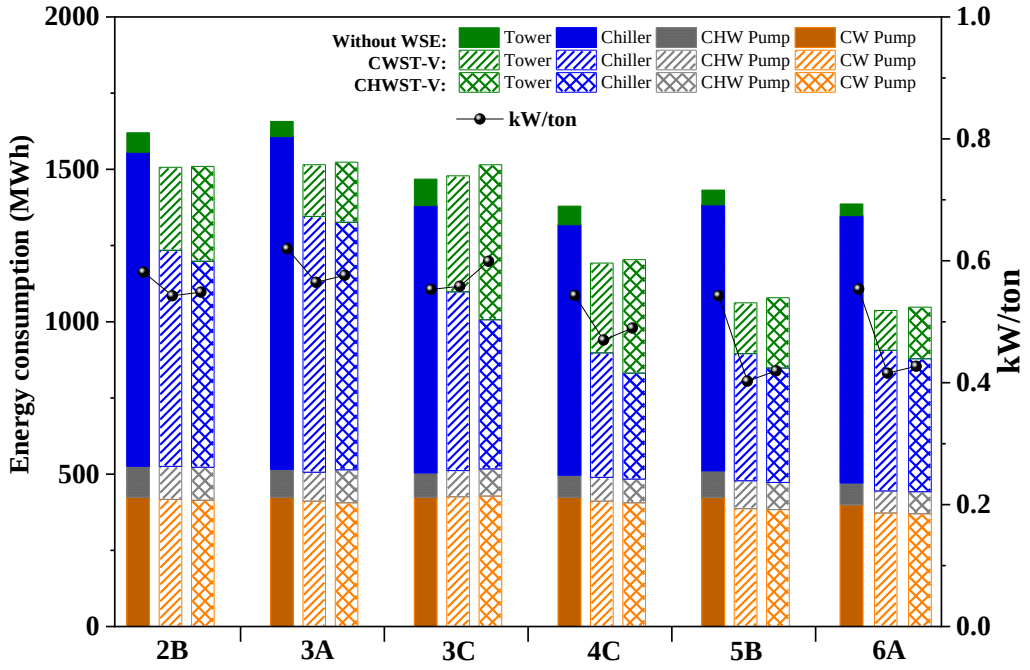

Fig. 10. Energy consumption of chiller plant with WSE under variable load in six climates.

Fig. 11 shows the monthly kW/ton of chiller plant with WSE under variable load. The chiller plant kW/ton reaches the maximum value in July or August when monthly averaged T_{wb} is at its highest. For cold months (e.g., January, February, November, and December), the chiller plant kW/ton of the two sequences have no obvious differences. When the monthly averaged T_{wb} is above 12°C in hot months (e.g., June, July, and August), CWST-based control sequence has the least kW/ton in the six climates.

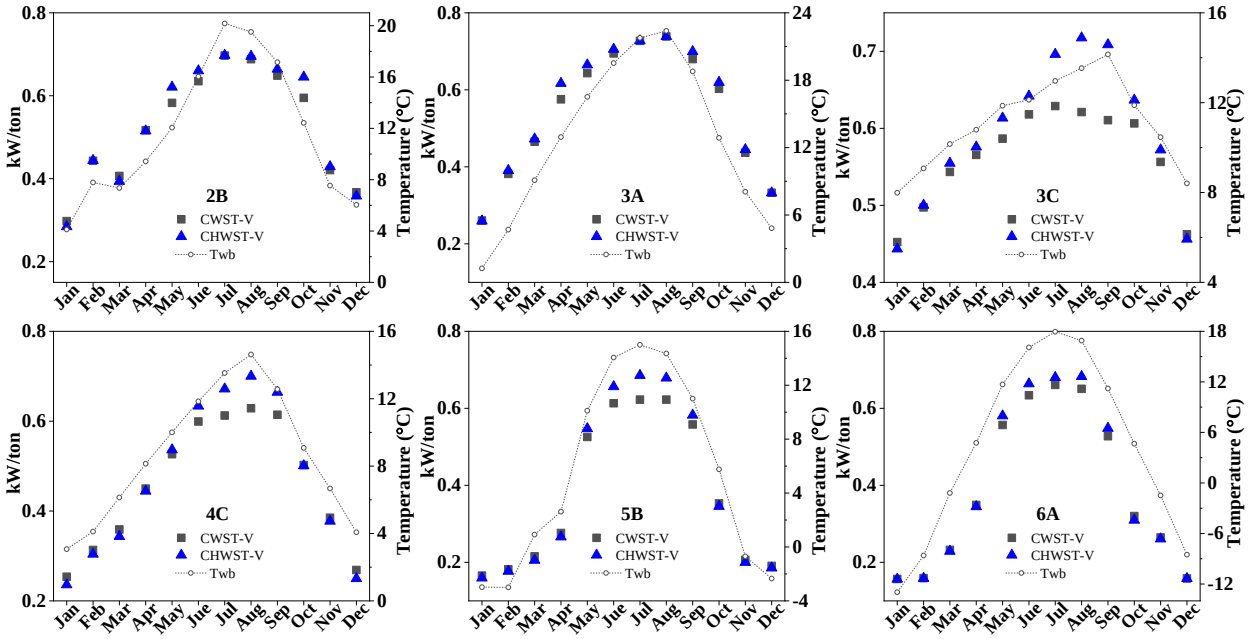

Fig. 11. Monthly chiller plant with WSE kW/ton under variable load.

5.2.4 Unexpected energy performance

The kW/ton of chiller plant with WSE usually reduces from FMC mode to PMC mode and FC mode since WSE can increase cooling efficiency by taking advantage of using free cooling. However, it is found that, in some scenarios, the chiller plant may require more energy: (1) in FC mode than PMC mode or (2) in PMC mode than FMC mode, which is contradictory to the above expectation. This section investigates and provides explanations for those phenomena. The first is chiller plant uses more energy in FC mode than in PMC mode. Fig. 12 (a) shows the energy performance details of the two sequences under variable load within one day (Jan 10). After 9 a.m., as shown in Fig. 12 (b), the cooling tower power of using CWST-based control in PMC mode is lower than the one using CHWST-based control in FC mode. This is because the maximum fan speed ratio is set as 95% in PMC mode and 100% in FC mode. The CW pumps also use less power since only one pump is activated in PMC mode, but two CW pumps are active at 100% speed ratio in FC mode. This leads to a power reduction of 22 kW with 10 kW from the cooling tower and 12 kW from CW pumps, which is more than the increased chiller power (5 kW - 17 kW). Thus, the chiller plant power in PMC mode is lower than the one in FC mode.

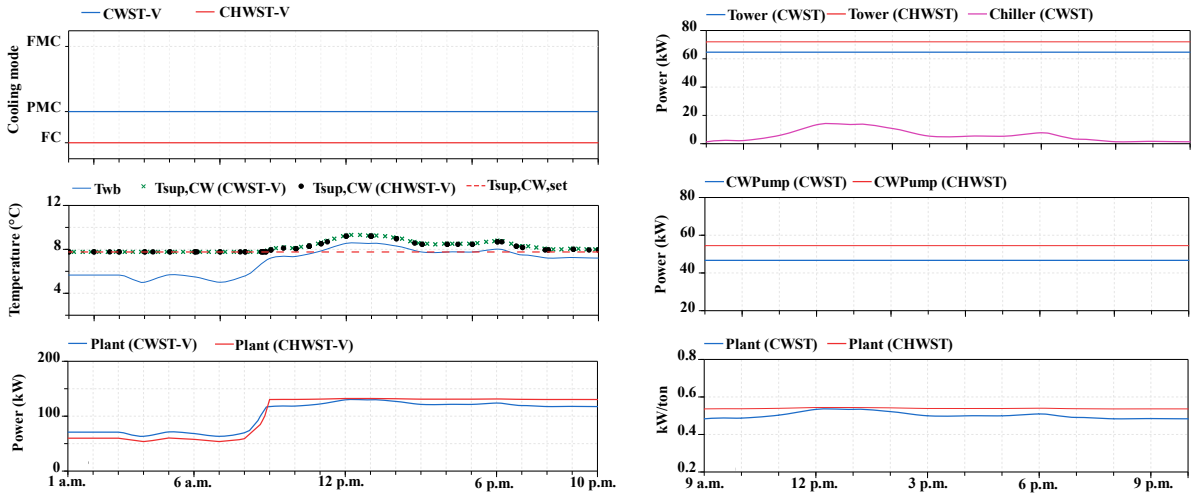

(a) Results from 1 a.m. to 10 p.m. (b) Details from 9 a.m. to 9 p.m.

Fig. 12. Details of energy performance in FC mode and PMC mode.

The second scenario is when the chiller plant kW/ton in PMC mode is higher than in FMC mode. Fig. 13 (a) shows the energy performance of CHWST-based control under constant load for one day (Aug 1). In PMC mode (at 8 a.m.), T_{wb} is 13.5 ˚C and $T_{sup,CW,set}$ is 7.8 ˚C, the cooling tower fan runs at the maximum speed 95%. The cooling tower and chiller power consumption are 65 kW and 242 kW, respectively. In FMC mode (at 12 p.m.), the cooling tower fan speed ratio gradually decreases from 95% to 63%. The power of the tower and chiller is 20 kW and 269 kW, respectively. As shown in Fig. 13 (b), the total power of the tower and chiller in PMC mode (307 kW) is higher than in FMC mode (289 kW). This result indicates $T_{sup,CW,set}$ is too low in this weather condition

so that the tower used more power (45 kW) than the savings from the chiller (27 kW). It is also found that using WSE requires more energy than using chiller-only when T_{wb} is above 11.8 ˚C. To reduce energy use for chiller plant, it is critical to balance energy use between towers and chillers by optimizing $T_{Sup,CW}$ set point.

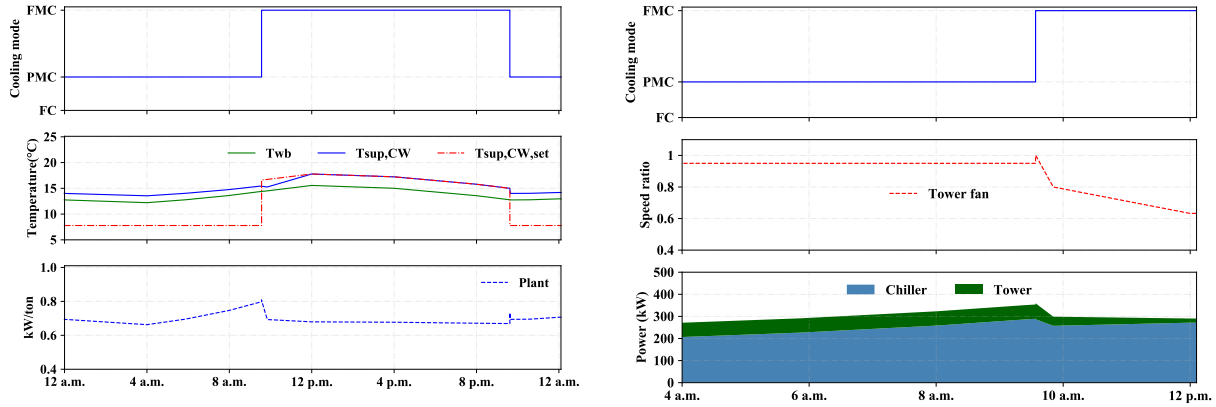

(a) Results from 12 a.m. to 12 a.m. (b) Details from 4 a.m. to 12 p.m.

Fig. 13. Details of energy performance in PMC mode and FMC mode.

6. Discussion

This study models a chiller plant with integrated WSE in parallel connection on the condenser water side, which is the most common configuration identified in the literature (as summarized in Appendix A). A total of 24 modeling scenarios, spanning two advanced control sequences, two cooling load types, and six climate zones, are included in this study to demonstrate the flexible and dynamic simulation capabilities of the developed system model. Under diverse climate conditions, the developed models reveal the system performances, from annual energy consumption to transient control responses. Many systems' performance results in terms of control stability and energy consumption are as expected. For example, the control indicator $T_{sup,CHW}$ drifts beyond the setpoint during FC mode due to the waiting time and dead band temperature adopted in the control sequences (e.g., waiting time 5 minutes and dead band 1.11 ˚C in Eq (6)); the chiller plant without WSE consumes notably more energy than all configurations with WSE (as shown in Fig. 8 and Fig. 10). However, this study reveals unexpected operating conditions in some cases. For example, the plant consumed more energy in FC mode at times than in PMC model (as shown in Fig. 12), due to the fan and pump switch settings and sizing conditions (e.g., maximum fan speed ratio is 100% in FC mode and 95% in PMC mode); the plant may consume more energy in PMC mode than in PMC model (as shown in Fig. 13), due to the tower using more power (e.g., 45 kW) than the savings from the chiller (e.g., 27 kW) when using the low $T_{Sup,CW}$ set point in PMC mode. This counterintuitive performance provides opportunities to improve control parameters in real-world system by means of computer simulations.

The flexibility of the developed models allows control engineers to test their sequences under realistic thermofluid scenarios; compare simulations across multiple climates, loads, and control settings; and identify new opportunities for energy efficiency and reliability improvements. There

are some limitations of this study. The energy performance of the cooling system is only validated using the energy data generated by EnergyPlus since the measured data is not available. In addition, this study did not pass judgment on the control performance of the selected control sequences for the chiller plant with WSE since the performance is based on only the studied system configuration, equipment sizing, weather condition, and cooling load profiles. In real practice, the chiller plant with WSE is designed and sized specifically for the target climate, and naturally, the system sizing significantly affects the overall energy performance.

The developed testbed can assess, optimize, and improve real-world chiller plants with WSE in future works. Impacts of any control strategy on system performance, such as control sequence, $T_{sup,CW}$ reset control [23], fan speed maximum control, and chiller staging control, can be also investigated using the existing model.

7. Conclusion

The system performance of chillers plants with WSE are usually evaluated based on the specific system configuration, control sequence, and load type. There is a lack of a flexible model to systematically evaluate the energy performance of chiller plants with WSE across multiple control scenarios. As such, the open-source Modelica models developed through this work aimed to fill this gap. The available flexibility and system performance of the developed system model are demonstrated by implementing 24 simulation cases, including two advanced control sequences, two cooling load types, and six climate zones.

Results show that the control stability indicators of the selected control sequences met the set points at most times, and some dynamic transient behaviors for $T_{sup,CHW}$ and T_{SA} are also present. For example, $T_{sup,CHW}$ drifts beyond the setpoint during FC mode due to the waiting time and dead band temperature adopted in the control sequences. The energy performance indicator *PF* (kW/ton) of the chiller plant with WSE usually decreases from FMC mode (*PF*=0.65) to PMC mode and FC mode (*PF*=0.22), since the WSE increases cooling efficiency by taking advantage of "free cooling". Additionally, the chiller plant with WSE consumes notably less energy than the plant without WSE. With WSE, the energy saving potential of a chiller plant using the selected control sequences varies from 8.6% to 36.8% under constant load profiles in six climates, while it varies from 6.3% to 25.8% under variable load profiles in most climates. Additionally, this study also reveals unexpected operating conditions. For example, there are some scenarios that the chiller plant with WSE requires more energy in PMC mode than in FMC mode, due to the fan and pump operating settings and sizing conditions. The reason for this counterintuitive performance is because the tower used more power (e.g., 45 kW) than the savings from the chiller (e.g., 27 kW) when using the low $T_{Sup,CW}$ set point in PMC mode, which provides opportunities to improve control parameters in real-world systems.

As seen above, a control sequence can occasionally cause unusual energy performance outputs in chiller plant with WSE and hence a comprehensive testbed with wide simulation capacity is much needed. The flexibility of the developed system models throughout this work allows control engineers to test their sequences under realistic thermofluid scenarios, compare simulations across multiple climates, loads, and control settings, and optimize chiller plants to reap their maximum

energy efficiency benefits across diverse control scenarios. This system model will be open-source released, allowing wide-scale adoption.

Acknowledgment

This paper is the outcome of the research project TRP-1661 sponsored by American Society of Heating, Refrigerating and Air-Conditioning Engineers (ASHRAE). The Chinese team was supported by National Natural Science Foundation of China (No. 52078146), Key Projects of Basic Research and Applied Basic Research of Universities in Guangdong Province (No. 2018KZDXM050), Science and Technology Project of Guangdong Province (No. 2016A010104022).

Appendix

A. System configuration

Table 7 shows configuration of the chiller and WSE connections.

Table 7 Chiller and WSE connections mentioned in the literature.

Reference	System	Chiller-WSE connection on chilled water side	Chiller-WSE connection on condenser water side	No. of chillers	No. of WSE
[5]	Primary- secondary	Nonintegrated	Parallel	1	1
[7]	Primary-only	Integrated on load side	Parallel	2	1
	Primary-only	Nonintegrated	Parallel	2	1
[8]	N/A	Integrated	Parallel	N/A	N/A
		Nonintegrated	Parallel	N/A	N/A
[9]	Primary-only	Integrated on load side	Parallel	2	1
	Primary-secondary	Integrated on load side	Parallel	2	1
	Primary-secondary	Nonintegrated	Parallel	2	1
[19]	Primary-only	Integrated on plant side	Parallel	1	1
[20]	Primary-secondary	Integrated	Series	3	1
[21]	Primary-secondary	Nonintegrated	Parallel	6	1
[22]	Primary-only	Nonintegrated	Parallel	8	N/A
[26]	Primary-only	Integrated on plant side	Series	N/A	1
[28]	Primary-only	Integrated on load side	Series	1	1
[33]	Primary-only	Integrated on plant side	Parallel	4	4
[39]	Primary-secondary	Integrated on load side	Series	2	1
[43]	Primary- secondary	Integrated on plant side	Series	4	1

[44]	Primary-only	Integrated on load side	Parallel	N/A	N/A
[45]	Primary-only	Nonintegrated	Parallel	N/A	N/A
		Integrated on load side	Series	N/A	N/A
[46]	Primary-only	N/A	N/A	9	9
[47]	Primary-secondary	Integrated and nonintegrated in one system	Parallel	4	2

B. System sizing

Table 8 shows the plant's equipment sizing.

Table 8 Equipment sizing.

Equipment	Number	Equipment information	Parameter	Unit	Value
Chiller	2	Nominal capacity		kW	1294
		Design COP		-	7.61
		Evaporator	Flow rate	m^3/s	0.03243
			Pressure loss	kPa	44.8
		Condenser	Flow rate	m^3/s	0.04732
			Pressure loss	kPa	46.2
		Compressor	Number	-	1
			Speed type	Variable speed	
			Power	kW	170
WSE	1	Nominal capacity		kW	2588
		Chilled water side	Flow rate	m^3/s	0.09464
			Pressure loss	kPa	44.8
		Condenser water side	Flow rate	m^3/s	0.09464
			Pressure loss	kPa	46.2
		Design approach temperature		$^{\circ}C$	1.67
Chilled water pump	2	Head		kPa	584
		Power		kW	39.5
		Flow rate		m^3/s	0.04732
		Speed type		Variable speed	
Condenser water pump	2	Head		kPa	242
		Power		kW	46.7
		Flow rate		m^3/s	0.09464
		Speed type		Variable speed	
Cooling tower	2	Nominal capacity		kW	1460
		Design approach temperature		$^{\circ}C$	2.2
		Number of cells		-	1
		Number of fans		-	1
		Fan speed type		Variable speed	

C. Selected control sequences

C.1. CWST-based control

See Fig. 14 for the state graph of the CWST-based control sequence.

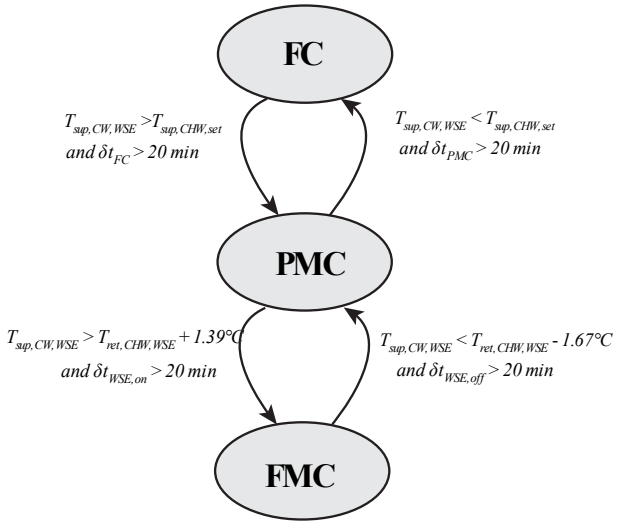

Fig. 14. State graph of a condenser water supply temperature (CWST)-based control sequence.

The cooling system will be controlled by the following logic:

(1) The transition from FC to PMC mode can be expressed as:

$$T_{sup,CW,WSE} > T_{sup,CHW,set} \; and \; \delta t_{FC} > 20min, \tag{2}$$

where $T_{sup,CW,WSE}$ is the condenser water supply temperature upstream of the WSE, $T_{sup,CHW,set}$ is the chilled water supply temperature set point, and δt_{FC} is the elapsed time of FC mode since the last activation. The waiting time threshold is 20 min, which is adjustable according to engineering practice.

(2) The transition from PMC to FMC mode is expressed as:

$$T_{sup,CW,WSE} > T_{ret,CHW,WSE} + 1.39℃ \; and \; \delta t_{WSE,on} > 20min, \tag{3}$$

where $T_{sup,CW,WSE}$ is the condenser water supply temperature upstream of the WSE, $T_{ret,CHW,WSE}$ is the chilled water return temperature upstream of the WSE, 1.39˚C (2.5˚F) is dead band differential temperature, and $\delta t_{WSE,on}$ is the elapsed time since the WSE was on.

(3) The transition from FMC to PMC mode is expressed as:

$$T_{sup,CW,WSE} < T_{ret,CHW,WSE} - 1.67℃ \; and \; \delta t_{WSE,off} > 20min, \tag{4}$$

where $T_{sup,CW,WSE}$ is the condenser water supply temperature upstream of the WSE, $T_{ret,CHW,WSE}$ is the chilled water return temperature upstream of the WSE, 1.67˚C (3˚F) is dead band differential temperature, and $\delta t_{WSE,off}$ is the elapsed time since the WSE was disabled.

(4) Lastly, the transition from PMC to FC mode is shown as:

$$T_{sup,CW,WSE} < T_{sup,CHW,set} \; and \; \delta t_{PMC} > 20min, \tag{5}$$

where $T_{sup,CW,WSE}$ is the condenser water supply temperature upstream of the WSE, $T_{sup,CHW,set}$ is the chilled water supply temperature set point, and δt_{PMC} is the run time of PMC mode since the last activation. Each of these waiting times helps avoid short cycling of the equipment.

C.2. CHWST-based control

See Fig. 15 for the state graph of the CHWST-based control sequence.

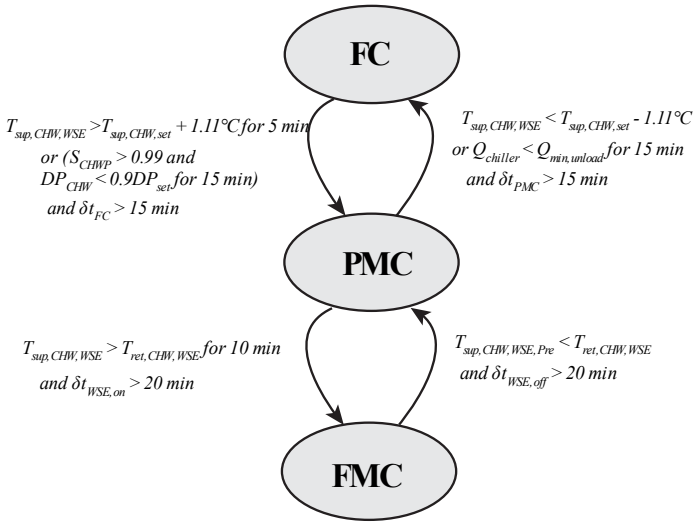

Fig. 15. State graph of a chilled water supply temperature (CHWST)-based control sequence.

The cooling system wills be controlled by the following logic:

(1) The transition from FC to PMC is expressed as:

$$\begin{gathered} T_{sup,CHW,WSE} > T_{sup,CHW,set} + 1.11℃ \text{ for } 5\ min \\ \left(S_{CHWP} > 99\% \text{ and } DP_{CHW} < 0.9 * DP_{CHW,set} \text{ for } 15min\right) \\ \text{and } \delta t_{FC} > 15min, \end{gathered} \tag{6}$$

where $T_{sup,CHW,WSE}$ is the chilled water supply temperature downstream of the WSE, $T_{sup,CHW,set}$ is the chilled water supply temperature set point, 1.11˚C (2˚F) is dead band differential temperature, S_{CHWP} is the speed of chilled water pumps, DP_{CHW} is the measured pressure drop of the chilled water loop, and $DP_{CHW,set}$ is the pressure drop set point of the chilled water loop.

(2) The transition from PMC to FMC mode is expressed as:

$$T_{sup,CHW,WSE} > T_{ret,CHW,WSE} \; for \; 10 \; min \tag{7}$$

$$and\ \delta t_{WSE,on} > 20\ min,$$

where $T_{sup,CHW,WSE}$ is the chilled water supply temperature downstream of the WSE, $T_{ret,CHW,WSE}$ is the chilled water return temperature upstream of the WSE, and $\delta t_{WSE,on}$ is the elapsed time since the WSE was on.

(3) The transition from FMC to PMC mode is expressed as:

$$\begin{gathered} T_{sup,CHW,WSE,pre} < T_{ret,CHW,WSE} \\ and\ \delta t_{WSE,off} > 20\ min, \end{gathered} \tag{8}$$

where $T_{ret,CHW,WSE}$ is the chilled water return temperature upstream of the WSE, $\delta t_{WSE,off}$ is the elapsed time since the WSE was disabled, $T_{sup,CHW,WSE,pre}$ is the predicted chilled water supply temperature downstream of the WSE, which can be predicted using an approximation algorithm, such as:

$$T_{sup,CHW,WSE,pre} = 0.9 * T_{wb} + T_{app,CT,pre} + T_{app,WSE,pre}, \tag{9}$$

where T_{wb} is outdoor air wet-bulb temperature, and $T_{app,CT,pre}$ is the predicted approach temperature in cooling towers, which can be a fixed or variable value. Here the designed approach temperature of cooling towers is set as 2.22 ˚C (4˚F) [18,48]. $T_{app,WSE,pre}$ is the predicted approach temperature of the WSE. Here a design approach temperature for WSE is set as 1.67˚C (3˚F) [7].

(4) The transition from PMC to FC mode is expressed as:

$$\begin{gathered} (T_{sup,CHW,WSE} < T_{sup,CHW,set} - 1.11℃ \\ or\ Q_{chiller} < Q_{chiller,unload,min})\ for\ 15\ min \\ and\ \delta t_{PMC} > 15\ min, \end{gathered} \tag{10}$$

where $T_{sup,CHW,WSE}$ is the chilled water supply temperature downstream of the WSE, $T_{sup,CHW,set}$ is the chilled water supply temperature set point, $Q_{chiller}$ is the current cooling load in the chiller, $Q_{chiller,unload,min}$ is the minimum unload cooling load of the chiller.

Reference

[1] Jia L, Liu J, Wei S, Xu J. Study on the performance of two water-side free cooling methods in a semiconductor manufacturing factory. Energy Build 2021;243:110977.

[2] Amado EA, Schneider PS, Bresolin CS. Free cooling potential for Brazilian data centers based on approach point methodology. Int J Refrig 2021;122:171–80.

[3] Fu Y, Zuo W, Wetter M, VanGilder JW, Yang P. Equation-based object-oriented modeling and simulation of data center cooling systems. Energy Build 2019;198:503–19.

[4] Deymi-Dashtebayaz M, Namanlo SV. Potentiometric and economic analysis of using air and water-side economizers for data center cooling based on various weather conditions. Int J Refrig 2019;99:213–25.

[5] Díaz AJ, Cáceres R, Torres R, Cardemil JM, Silva-Llanca L. Effect of climate conditions on the thermodynamic performance of a data center cooling system under water-side economization. Energy Build 2020;208:109634.

[6] Hong T, Yang L, Hill D, Feng W. Data and analytics to inform energy retrofit of high performance

buildings. Appl Energy 2014;126:90–106.
[7] Taylor ST. How to design & control waterside economizers. ASHRAE J 2014;56:30–6.
[8] Lui YY. Waterside and airside economizers design considerations for data center facilities. ASHRAE Trans 2010;116(1):98–108.
[9] Stein J. Waterside economizing in data centers: design and control considerations. ASHRAE Trans 2009;115(2):192–200.
[10] Huang S, Zuo W, Sohn MD. Improved cooling tower control of legacy chiller plants by optimizing the condenser water set point. Build Environ 2017;111:33–46.
[11] Beaty DL, Quirk D, Morrison FT. Designing data center waterside economizers part 2: optimizing the design. ASHRAE J 2019;61:78–86.
[12] Gozcu O, Ozada B, Carfi MU, Erden HS. Worldwide energy analysis of major free cooling methods for data centers. Proc. 16th Intersoc. Conf. Therm. Thermomechanical Phenom. Electron. Syst. ITherm 2017, Orlando, FL, USA: IEEE; 2017;968–76.
[13] Huang P, Copertaro B, Zhang X, Shen J, Löfgren I, Rönnelid M, et al. A review of data centers as prosumers in district energy systems: Renewable energy integration and waste heat reuse for district heating. Appl Energy 2020;258.
[14] Wetter M. A view on future building system modeling and simulation. Build. Perform. Simul. Des. Oper., 2011;481–505.
[15] Donida F, Ferretti G, Savaresi SM, Tanelli M. Object-oriented modelling and simulation of a motorcycle. Math Comput Model Dyn Syst 2008;14:79–100.
[16] Wetter M, Zuo W, Nouidui TS, Pang X. Modelica buildings library. J Build Perform Simul 2014;7:253–70.
[17] Wetter M, Bonvini M, Nouidui TS, Tian W, Zuo W. Modelica buildings library 2.0. 14th Int. Conf. IBPSA - Build. Simul. 2015, Hyderabad, India: 2015;387–94.
[18] Beaty DL, Quirk D, Morrison FT. Designing data center waterside economizers part 1: tower sizing. ASHRAE J 2019;61:78–86.
[19] Ham SW, Jeong JW. Impact of aisle containment on energy performance of a data center when using an integrated water-side economizer. Appl Therm Eng 2016;105:372–84.
[20] Duda SW. Waterside economizer retrofit for data center. ASHRAE J 2017;59:58–69.
[21] Jaramillo R, Jeon B, Braun JE, Horton WT, Schuster D. Simulation assessment of free-cooling technology for a large campus. ASHRAE Trans 2015;121:471–86.
[22] Kim JY, Chang HJ, Jung YH, Cho KM, Augenbroe G. Energy conservation effects of a multi-stage outdoor air enabled cooling system in a data center. Energy Build 2017;138:257–70.
[23] Li J, Li Z. Model-based optimization of free cooling switchover temperature and cooling tower approach temperature for data center cooling system with water-side economizer. Energy Build 2020;227:110407.
[24] Jorissen F, Wetter M, Helsen L. Simplifications for hydronic system models in modelica. J Build Perform Simul 2018;11:639–54.
[25] Fu Y, Wetter M, Zuo W. Modelica models for data center cooling systems. 2018 Build Perform Anal Conf 2018:438–45.
[26] Wei D, Li B, Shi Y, Li Z. Energy-efficient mode transition strategies of data center cooling systems. Int J Simul Syst Sci Technol 2016;17:26.1-26.6.
[27] Agrawal A, Khichar M, Jain S. Transient simulation of wet cooling strategies for a data center in worldwide climate zones. Energy Build 2016;127:352–9.
[28] Durand-Estebe B, Le Bot C, Mancos JN, Arquis E. Simulation of a temperature adaptive control strategy for an IWSE economizer in a data center. Appl Energy 2014;134:45–56.
[29] Wetter M, Bonvini M, Nouidui TS. Equation-based languages - a new paradigm for building energy modeling, simulation and optimization. Energy Build 2016;117:290–300.
[30] Wetter M, Haugstetter C. Modelica versus TRNSYS–A comparison between an equation-based and a procedural modeling language for building energy simulation. Proc SimBuild 2006;2.

[31] Kim D, Zuo W, Braun JE, Wetter M. Comparisons of building system modeling approaches for control system design. Proc. BS 2013 13th Conf. Int. Build. Perform. Simul. Assoc., 2013;3267–74.
[32] Wetter M. Modelica-based modelling and simulation to support research and development in building energy and control systems. J Build Perform Simul 2009;2:143–61.
[33] Cheung H, Wang S. Optimal design of data center cooling systems concerning multi-chiller system configuration and component selection for energy-efficient operation and maximized free-cooling. Renew Energy 2019;143:1717–31.
[34] Shah P, Tailor N. Merkel's method for designing induced draft cooling tower. Int J Adv Res Eng Technol 2015;6:63–70.
[35] Guo Q, Qi X, Wei Z, Sun P. An analytical approach to wet cooling towers based on functional analysis. Math Probl Eng 2019;2019:9.
[36] EnergyPlus version 9.3.0 documentation: engineering reference. U.S. Department of Energy; 2020.
[37] Taylor ST. Optimizing design & control of chilled water plants: part 5: optimized control sequences. ASHRAE J 2011;53:14–25.
[38] Fu Y, Lu X, Zuo W. Modelica Models for the Control Evaluations of Chilled Water System with Waterside Economizer. Proc. 13th Int. Model. Conf. Regensburg, Ger. 2019, vol. 157, 2019, p. 811–8.
[39] Griffin B. Honorable mention: industrial facilities or processes, new Data Center: economizer efficiency. ASHRAE J 2015;57:64–70.
[40] Fu Y, Zuo W, Wetter M, VanGilder JW, Han X, Plamondon D. Equation-based object-oriented modeling and simulation for data center cooling: a case study. Energy Build 2019;186:108–25.
[41] Karami M, Wang L. Particle swarm optimization for control operation of an all-variable speed water-cooled chiller plant. Appl Therm Eng 2018;130:962–78.
[42] Hartman T. All-variable speed centrifugal chiller plants. ASHRAE J 2001;43:43–53.
[43] Li J, Jurasz J, Li H, Tao WQ, Duan Y, Yan J. A new indicator for a fair comparison on the energy performance of data centers. Appl Energy 2020;276:115497.
[44] Comperchio D, Behere S. Theoretical and Empirical Energy Impacts of Economization in Data Centers. Proc. ASME 2015 Int. Tech. Conf. Exhib. Packag. Integr. Electron. Photonic, Microsystems, 2015, San Fr. California, USA, American Society of Mechanical Engineers; 2015.
[45] Newsletter CE. Carrier Engineering Newsletter How to Model a Waterside Economizer Application 2016;4:1–16.
[46] Cho J, Yang J, Lee C, Lee J. Development of an energy evaluation and design tool for dedicated cooling systems of data centers: sensing data center cooling energy efficiency. Energy Build 2015;96:357–72.
[47] Greeley DG. The winter efficiency protagonist: best practice for a partial waterside economizer. Eng Syst 2006;23:68–76.
[48] Schwedler M. Effect of heat rejection load and wet bulb on cooling tower performance. ASHRAE J 2014;56:16–22.